



ELSEVIER

Physica E 12 (2002) 802–805

**PHYSICA**

www.elsevier.com/locate/physce

# Mapping the $g$ factor anisotropy of InAs self-assembled quantum dots

I. Hapke-Wurst<sup>a,\*</sup>, U. Zeitler<sup>a</sup>, R.J. Haug<sup>a</sup>, K. Pierz<sup>b</sup><sup>a</sup>*Institut für Festkörperphysik, Universität Hannover, Appelstraße 2, 30167 Hannover, Germany*<sup>b</sup>*Physikalisch-Technische Bundesanstalt Braunschweig, Bundesallee 100, 38116 Braunschweig, Germany*

---

## Abstract

We use magneto-tunneling spectroscopy to investigate the Landé  $g$  factor of single self-assembled InAs quantum dots. With increasing ground state energy we find an increase of  $g$ . For different orientations of the magnetic field with respect to the crystallographic axes we mapped the anisotropy of the effective electron  $g$  factor. In addition to the strong anisotropy for tilting the field from the growth direction  $[1\ 0\ 0]$  into the direction  $[0\ \bar{1}\ \bar{1}]$  a smaller, but measurable anisotropy is detected for changing the magnetic field direction from  $[0\ \bar{1}\ \bar{1}]$  to  $[0\ \bar{1}\ 1]$ . © 2002 Elsevier Science B.V. All rights reserved.

*PACS:* 73.23.Hk; 73.40.Gk; 73.63.Kv*Keywords:* Resonant tunneling;  $g$  factor; Self-assembled InAs dots

---

## 1. Introduction

Over the last few years several groups probed the electronic properties of self-assembled InAs quantum dots (QDs) in resonant tunneling experiments [1]. In magnetotransport measurements the degeneracy of the QD states is lifted and it is possible to resolve distinct spin states at low temperatures [2]. Here we present results of magneto-tunneling experiments concerning the Landé  $g$  factor of self-assembled InAs quantum dots. We examined the influence of the ground state energies of the dots on the magnitude of  $g$  for different InAs dots and the dependence of  $g$  on the crystallographic directions.

## 2. Magnetotunneling

Our samples were prepared by molecular beam epitaxy using a resonant tunneling diode design on a  $50\ \mu\text{m}$  square mesa. A layer of self-assembled InAs QDs as active area is embedded in a 10 nm AlAs barrier and highly doped three-dimensional GaAs electrodes. Growth details are given in Ref. [3]. The structure and size of the InAs QDs have been analyzed by transmission electron microscope (TEM) and atomic force microscope (AFM) measurements. The results of both methods give us a dot size of about 10–15 nm in diameter and 4 nm in height and a dot density of  $1000\ \mu\text{m}^{-2}$ .

The transport measurements on the QD samples were made at low temperatures of 0.1 and 1.3 K. A bias applied on the electrodes shifts the emitter Fermi energy with respect to the discrete energy levels of the InAs dots. Resonant tunneling

---

\* Corresponding author. Fax: +49-(0)511-762-2904.

E-mail address: wurst@nano.uni-hannover.de  
(I. Hapke-Wurst).

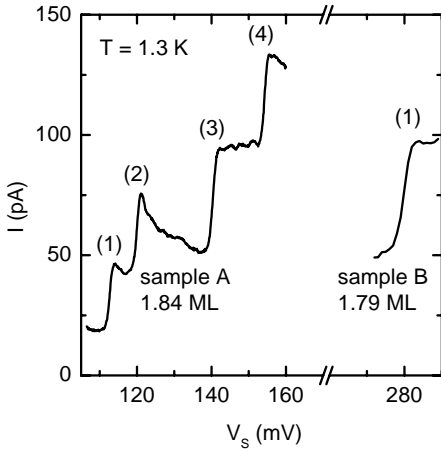


Fig. 1.  $I$ - $V$ -characteristics for different dots at  $T = 1.3$  K. Sample A contains 1.84 ML InAs, sample B contains 1.79 ML InAs.

from the three-dimensional emitter through the zero-dimensional dot levels leads to steps in the current-voltage ( $I$ - $V$ )-characteristics. Typical step heights are a few tens of pA as shown in Fig. 1.

Step (1) of sample A, which contains nominally 1.84 monolayers (ML) InAs, represents tunneling through the ground state of one dot. The successive steps (2)–(4) at higher onset voltages  $V_S$  result from tunneling through other dots with slightly increasing ground state energies. The comparison with sample B, which contains a thinner InAs coverage of 1.79 ML, shows a higher onset voltage  $V_S$  and a higher ground state energy for the first step labeled (1). We correlate this increase in the ground state energy with an increase in the energy gap  $E_0$  between valence band holes and conduction band electrons and a decrease in the QD size. In order to verify our findings we compared our tunneling data with photoluminescence (PL) spectra and AFM measurements on uncapped reference samples [4]. All samples were grown with variable InAs coverage, which is strongly correlated with the dot size. We observed a clear dependence of the energy position of the PL peak as well as the voltage position of the tunneling steps on the InAs coverage. For low coverage the PL emission peak, which represents transitions between conduction band and valence band states, is at  $E_0 = 1.9$  eV. The corresponding dot size deduced from the AFM data is  $\approx 10$  nm. With increasing InAs coverage the posi-

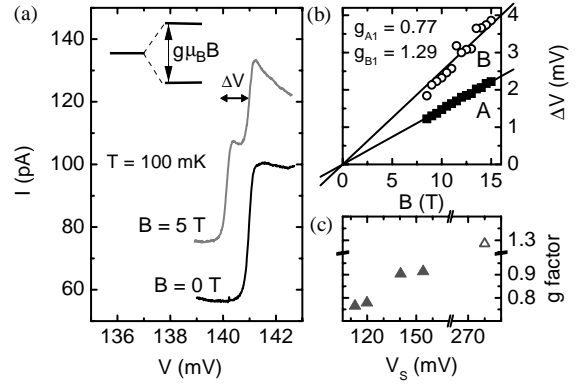


Fig. 2.  $I$ - $V$ -characteristics of a single step at magnetic fields  $B = 0$  and 5 T applied in the growth plane. Inset: Sketch of the Zeeman splitting of a dot state. (b) Voltage difference  $\Delta V$  due to spin splitting for the first steps of samples A and B in Fig. 1 as a function of the magnetic field  $B \parallel [0 \bar{1} 1]$  (see Fig. 3). (c)  $g$  factor in dependence of the voltage position of the steps for  $B \parallel [0 \bar{1} 1]$ .

tion of the PL peak shifts to lower energies down to  $E_0 = 1.6$  eV for  $\approx 14$  nm-dots. This redshift due to lower ground state energies in larger dots is in agreement with our tunneling data showing lower onset voltages for the current steps.

### 3. Influence of the dot size on the $g$ factor

In a magnetic field the spin degeneracy of the dot energy levels is lifted. The energy difference between the spin levels is  $\Delta E = g\mu_B B$  as sketched in Fig. 2. In the  $I$ - $V$ -curves we observe a splitting of each step into two separate steps with a voltage difference  $\Delta V$ . The linear increase of  $\Delta V$  with the magnetic field is characteristic for Zeeman splitting. Fig. 2(a) shows a spin split step at  $B = 5$  T for a magnetic field applied in the growth plane. By analyzing the energy difference  $\Delta E = \alpha e \Delta V$  with  $\alpha \approx 0.3$  a lever factor indicating the voltage drop over the relevant barrier we can determine the  $g$  factor for each dot. We deduced  $\alpha$  from temperature dependent measurements on the step edges.

In Fig. 2(b) the voltage difference  $\Delta V$  in a magnetic field  $B \parallel [0 \bar{1} 1]$  is plotted exemplarily for step (1) of samples A and B. The corresponding  $g$  factors are  $g_{A1} = 0.77$  and  $g_{B1} = 1.29$ , respectively. We observe an increase in the value of  $g$  for increasing voltage

positions of the steps as shown in Fig. 2(c) for  $B \parallel [0\bar{1}1]$ . From temperature dependent measurements we determined the sign of  $g$  as positive [5]. These values differ strongly from the value of bulk InAs. To explain qualitatively our results we apply a formula based on a  $\mathbf{k} \cdot \mathbf{p}$  model [6,7]

$$g^* = g_0 - \frac{2P^2}{3} \frac{\Delta_0}{E_0(E_0 + \Delta_0)},$$

with  $g_0 = 2$ ,  $P^2 = 22.2$  eV the interband matrix element for InAs,  $\Delta_0 = 0.38$  eV the valence-band spin-orbit splitting for InAs. The energy gap between valence band electrons and conduction band holes is in the range  $E_0 = 1.55$ – $1.66$  eV for our dots deduced from PL data. With this values we calculate a  $g$  factor in the range  $g^* = 0.12$ – $0.34$ . As the model does not include strain and other effects, for example AlAs alloying into the dots, the consistency between the calculated and the experimentally determined  $g$  is adequate, especially for taking into account the  $g$  factor of  $g^* = -15$  for bulk InAs. The  $\mathbf{k} \cdot \mathbf{p}$  model helps also to explain the influence of the dot size on the  $g$  factor value. A decreasing dot size leads to an increasing energy gap  $E_0$  as shown above. An increasing energy  $E_0$  leads to values of  $g^*$  approaching  $g_0$ , as observed in our experiment.

#### 4. $g$ Factor anisotropy

In order to determine the  $g$  factor for different crystallographic axes we measured  $I$ – $V$ -characteristics at a fixed field of 15 T and tilted the sample in the magnetic field. For a magnetic-field turn from the growth plane  $[0\bar{1}\bar{1}]$  into the growth axis  $[100]$ , we observe an increase in  $g$  of 30% for several samples [8]. We attribute this strong anisotropy to the shape of InAs dots embedded in the AlAs barrier. Our measurements also cover different angles of the magnetic field in the growth plane, i.e. the base plane of the InAs QDs. Tilting the field from  $[0\bar{1}\bar{1}]$  to  $[0\bar{1}1]$  the  $g$  factor exhibits a decrease of  $\sim 10\%$  hinting at the anisotropy of the system as shown in Fig. 3. These findings can be described by the phenomenological formula [7]

$$g^*(\varphi) = \sqrt{g_{[0\bar{1}\bar{1}]}^2 \cos^2 \varphi + g_{[0\bar{1}1]}^2 \sin^2 \varphi}.$$

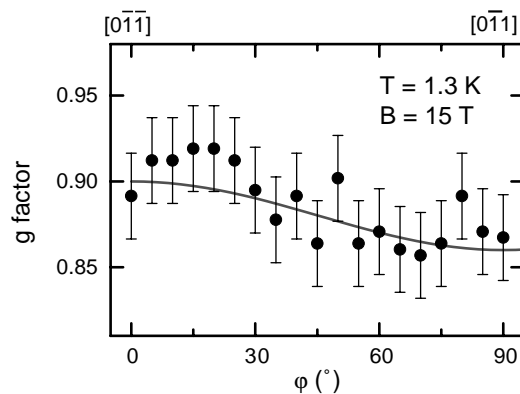


Fig. 3.  $g$  factor for different orientations of the magnetic field with respect to the crystallographic axes. The angle  $\varphi$  represents angles in the growth plane.

The solid line in Fig. 3 shows the calculated  $g^*$  with  $g_{[0\bar{1}\bar{1}]} = 0.90$  and  $g_{[0\bar{1}1]} = 0.86$  for this specific dot. For  $B \parallel [0\bar{1}\bar{1}]$   $g$  is larger than for  $B \parallel [0\bar{1}1]$  for all the dots investigated.

#### 5. Conclusions

We have studied the Landé  $g$  factor in self-assembled InAs QDs. The  $g$  factor shows a clear dependence on the energy gap between valence band holes and conduction band electrons which we correlate to the dot size. For an increasing energy gap  $g$  increases. In tilted magnetic fields we mapped the anisotropy of the  $g$  factor in the growth plane and observed a decrease of the  $g$  factor when tilting the field from  $[0\bar{1}\bar{1}]$  to  $[0\bar{1}1]$ .

#### Acknowledgements

Matter Part of this work has been supported by the DFG (HA 1826/5-1). We thank P. Hinze for TEM and U.F. Keyser for AFM.

#### References

- [1] I.E. Itskevich, T. Ihn, A. Thornton, M. Henini, T.J. Foster, P. Moriarty, A. Nogaret, P.H. Beton, L. Eaves, P.C. Main, Phys. Rev. B 54 (1996) 16401;

- T. Suzuki, K. Nomoto, K. Taira, I. Hase, *Jpn. J. Appl. Phys.* 36 (1997) 1917;  
M. Narihiro, G. Yusa, Y. Nakamura, T. Noda, H. Sakaki, *Appl. Phys. Lett.* 70 (1997) 105.
- [2] A.S.G. Thornton, T. Ihn, P.C. Main, L. Eaves, M. Henini, *Appl. Phys. Lett.* 73 (1998) 354.
- [3] I. Hapke-Wurst, U. Zeitler, H.W. Schumacher, R.J. Haug, K. Pierz, F.J. Ahlers, *Semicond. Sci. Technol.* 14 (1999) L41.
- [4] K. Pierz, Z. Ma, I. Hapke-Wurst, U.F. Keyser, U. Zeitler, R.J. Haug, *Physica E*, to be published.
- [5] I. Hapke-Wurst, U. Zeitler, H. Frahm, A.G.M. Jansen, R.J. Haug, K. Pierz, *Phys. Rev. B* 62 (2000) 12621.
- [6] C. Hermann, C. Weisbuch, *Phys. Rev. B* 15 (1977) 823.
- [7] A.A. Kiselev, E.L. Ivchenko, U. Rössler, *Phys. Rev. B* 58 (1998) 16353.
- [8] J.-M. Meyer, I. Hapke-Wurst, U. Zeitler, R.J. Haug, K. Pierz, *Phys. Status Solidi B* 224 (2001) 685.